

# Neutron skin thickness of $^{208}\text{Pb}$ determined from reaction cross section for proton scattering

Shingo Tagami, Tomotsugu Wakasa, Jun Matsui, and Masanobu Yahiro\*  
*Department of Physics, Kyushu University, Fukuoka 819-0395, Japan*

Maya Takechi  
*Niigata University, Niigata 950-2181, Japan*  
(Dated: October 28, 2021)

**Background:** The reaction cross section  $\sigma_R$  is useful to determine the neutron radius  $R_n$  as well as the matter radius  $R_m$ . The chiral (Kyushu)  $g$ -matrix folding model for  $^{12}\text{C}$  scattering on  $^9\text{Be}$ ,  $^{12}\text{C}$ ,  $^{27}\text{Al}$  targets was tested in the incident energy range of  $30 \leq E_{\text{in}} \leq 400$  MeV, and it is found that the model reliably reproduces the  $\sigma_R$  in  $30 \leq E_{\text{in}} \leq 100$  MeV and  $250 \leq E_{\text{in}} \leq 400$  MeV.

**Aim:** We determine  $R_n$  and the neutron skin thickness  $R_{\text{skin}}$  of  $^{208}\text{Pb}$  by using high-quality  $\sigma_R$  data for the  $p + ^{208}\text{Pb}$  scattering in  $30 \leq E_{\text{in}} \leq 100$  MeV. The theoretical model is the Kyushu  $g$ -matrix folding model with the densities calculated with Gongny-D1S HFB (GHFB) with the angular momentum projection (AMP).

**Results:** The Kyushu  $g$ -matrix folding model with the GHFB+AMP densities underestimates  $\sigma_R$  in  $30 \leq E_{\text{in}} \leq 100$  MeV only by a factor of 0.97. Since the proton radius  $R_p$  calculated with GHFB+AMP agrees with the precise experimental data of 5.444 fm, the small deviation of the theoretical result from the data on  $\sigma_R$  allows us to scale the GHFB+AMP neutron density so as to reproduce the  $\sigma_R$  data. In  $E_{\text{in}} = 30\text{--}100$  MeV, the experimental  $\sigma_R$  data can be reproduced by assuming the neutron radius of  $^{208}\text{Pb}$  as  $R_n = 5.722 \pm 0.035$  fm.

**Conclusion:** The present result  $R_{\text{skin}} = 0.278 \pm 0.035$  fm is in good agreement with the recent PREX-II result of  $r_{\text{skin}} = 0.283 \pm 0.071$  fm.

## I. INTRODUCTION

Horowitz *et al.* [1] proposed a direct measurement for neutron skin  $R_{\text{skin}} = R_n - R_p$ , where  $R_n \equiv \langle r_n^2 \rangle^{1/2}$  and  $R_p \equiv \langle r_p^2 \rangle^{1/2}$  are the root-mean-square (rms) radii of point neutrons and protons, respectively. The measurement consists of parity-violating ( $PV$ ) and elastic electron scattering. The neutron radius  $R_n$  is determined from the former experiment, whereas the proton radius  $R_p$  is from the latter.

Very recently, by combining the original Lead Radius Experiment (PREX) result [2, 3] with the updated PREX-II result, the PREX collaboration reported the following value [4]:

$$R_{\text{skin}}^{PV} = 0.283 \pm 0.071 \text{ fm}, \quad (1)$$

where the quoted uncertainty represents a  $1\sigma$  error and has been greatly reduced from the original value of  $\pm 0.177$  fm (quadratic sum of experimental and model uncertainties) [3]. The  $R_{\text{skin}}^{PV}$  value is most reliable at the present stage, and provides crucial tests for the equation of state (EoS) of nuclear matter [5–9] as well as nuclear structure models. For example, Reed *et al.* [10] report a value of the slope parameter  $L$  of the EoS and examine the impact of such a stiff symmetry energy on some critical neutron-star observables. It should be noted that the  $R_{\text{skin}}^{PV}$  value is considerably larger than the other experimental values which are significantly model dependent [11–14]. As an exceptional case, a nonlocal dispersive-optical-model (DOM) analysis of  $^{208}\text{Pb}$  deduces  $r_{\text{skin}}^{\text{DOM}} = 0.25 \pm 0.05$  fm [15], which is consistent with  $R_{\text{skin}}^{PV}$ . It is the aim of this paper to present the  $R_{\text{skin}}$  value with a similar precision of  $R_{\text{skin}}^{PV}$  by analyzing the reaction cross section  $\sigma_R$  for  $p + ^{208}\text{Pb}$ .

The reaction cross section  $\sigma_R$  is a powerful tool to determine matter radius  $R_m$ . One can evaluate  $R_{\text{skin}}$  and  $R_n$  by using the  $R_m$  and the  $R_p$  [16] determined by the electron scattering. The  $g$ -matrix folding model is a standard way of deriving microscopic optical potential for not only proton scattering but also nucleus-nucleus scattering [17–27]. Applying the folding model with the Melbourne  $g$ -matrix [20] for interaction cross sections  $\sigma_I$  for Ne isotopes and  $\sigma_R$  for Mg isotopes, we discovered that  $^{31}\text{Ne}$  is a halo nucleus with large deformation [27], and deduced the matter radii  $r_m$  for Ne isotopes [28] and for Mg isotopes [29]. The folding potential is nonlocal, but is localized with the method of Ref. [17]. The validity is shown in Ref. [30]. For proton scattering, the localized version of  $g$ -matrix folding model [31] yields the same results as the full folding  $g$ -matrix folding model of Ref. [20], as shown by comparing the results of Ref. [31] with those of Ref. [20].

Recently, Kohno [32] calculated the  $g$ -matrix for the symmetric nuclear matter, using the Brueckner-Hartree-Fock method with chiral 4th-order ( $N^3\text{LO}$ ) nucleon-nucleon ( $NN$ ) forces (2NFs) and 3rd-order (NNLO) three-nucleon forces (3NFs). He set  $c_D = -2.5$  and  $c_E = 0.25$  so that the energy per nucleon can become minimum at  $\rho = \rho_0$ ; see Fig. 1 for  $c_D$  and  $c_E$ . Toyokawa *et al.* [25] localized the non-local chiral  $g$ -matrix into three-range Gaussian forms, using the localization method proposed by the Melbourne group [20, 33, 34]. The resulting local  $g$ -matrix is called “Kyushu  $g$ -matrix”.

The Kyushu  $g$ -matrix folding model is successful in reproducing  $\sigma_R$  and differential cross sections  $d\sigma/d\Omega$  for  $^4\text{He}$  scattering in  $E_{\text{in}} = 30\text{--}200$  MeV/nucleon [25]. The success is true for proton scattering at  $E_{\text{in}} = 65$  MeV [23]. Lately, we predicted neutron skin  $r_{\text{skin}}$  and proton, neutron, matter radii,  $R_p$ ,  $R_n$ ,  $R_m$  from interaction cross sections  $\sigma_I$  ( $\approx \sigma_R$ ) for  $^{42\text{--}51}\text{Ca} + ^{12}\text{C}$  scattering at  $E_{\text{in}} = 280$  MeV/nucleon, using the Kyushu  $g$ -matrix folding model with the densities calculated

\* orion093g@gmail.com

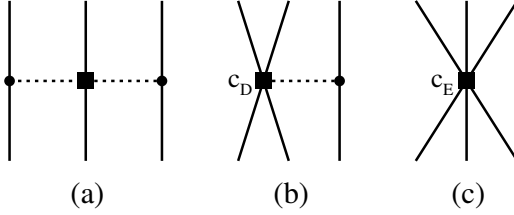


FIG. 1. 3NFs in NNLO. Diagram (a) corresponds to the Fujita-Miyazawa  $2\pi$ -exchange 3NF [35], and diagrams (b) and (c) correspond to  $1\pi$ -exchange and contact 3NFs. The solid and dashed lines denote nucleon and pion propagations, respectively, and filled circles and squares stand for vertices. The strength of the filled-square vertex is often called  $c_D$  in diagram (b) and  $c_E$  in diagram (c).

with Gongny-D1S HFB (GHFB) with and without the angular momentum projection (AMP) [26].

In Ref. [26], we tested the Kyushu  $g$ -matrix folding model for  $^{12}\text{C}$  scattering on  $^9\text{Be}$ ,  $^{12}\text{C}$ ,  $^{27}\text{Al}$  targets in  $30 \leq E_{\text{in}} \leq 400$  MeV, comparing the theoretical  $\sigma_R$  with the experimental data [36]. We found that the Kyushu  $g$ -matrix folding model is reliable for  $\sigma_R$  in  $30 \leq E_{\text{in}} \leq 100$  MeV and  $250 \leq E_{\text{in}} \leq 400$  MeV. This indicates that the Kyushu  $g$ -matrix folding model is applicable in  $30 \leq E_{\text{lab}} \leq 100$  MeV, although the data on  $p+^{208}\text{Pb}$  scattering are available in  $21 \leq E_{\text{lab}} \leq 180$  MeV.

In this paper, we present the determination of  $R_{\text{skin}}^{\text{GHFB}}$  from the measured  $\sigma_R$  for  $p+^{208}\text{Pb}$  scattering in  $30 \leq E_{\text{in}} \leq 100$  MeV [37–39], using the Kyushu  $g$ -matrix folding model with the GHFB+AMP densities. As mentioned above, the Kyushu  $g$ -matrix folding model is applicable in  $30 \leq E_{\text{in}} \leq 100$  MeV, although the data on  $p+^{208}\text{Pb}$  scattering are available in  $21 \leq E_{\text{in}} \leq 180$  MeV. In Sec. II, we briefly describe our model. Section III presents the results and a comparison with  $R_{\text{skin}}^{PV}$ , and discussion follows. Finally, Sec. IV is devoted to a summary.

## II. MODEL

Our model is the Kyushu  $g$ -matrix folding model [25] with the densities calculated with GHFB+AMP [26]. In Ref. [25], the Kyushu  $g$ -matrix is constructed from chiral interaction with the cutoff  $\Lambda = 550$  MeV. The model was tested for  $^{12}\text{C}$  scattering on  $^9\text{Be}$ ,  $^{12}\text{C}$ , and  $^{27}\text{Al}$  targets in  $30 \leq E_{\text{in}} \leq 400$  MeV. It is found that the Kyushu  $g$ -matrix folding model is good in  $30 \leq E_{\text{in}} \leq 100$  MeV and  $250 \leq E_{\text{in}} \leq 400$  MeV [26].

The brief formulation of the folding model itself is shown below. For nucleon-nucleus scattering, the potential is composed of the direct and exchange parts,  $U^{\text{DR}}$  and  $U^{\text{EX}}$  [29]:

$$U^{\text{DR}}(\mathbf{R}) = \sum_{\mu,\nu} \int \rho_T^\nu(\mathbf{r}_T) g_{\mu\nu}^{\text{DR}}(s; \rho_{\mu\nu}) d\mathbf{r}_T , \quad (2a)$$

$$U^{\text{EX}}(\mathbf{R}) = \sum_{\mu,\nu} \int \rho_T^\nu(\mathbf{r}_T, \mathbf{r}_T + \mathbf{s}) \times g_{\mu\nu}^{\text{EX}}(s; \rho_{\mu\nu}) \exp[-i\mathbf{K}(\mathbf{R}) \cdot \mathbf{s}/M] d\mathbf{r}_T \quad (2b)$$

where  $\mathbf{R}$  is the relative coordinate between a projectile (P) and a target (T),  $\mathbf{s} = -\mathbf{r}_T + \mathbf{R}$ , and  $\mathbf{r}_T$  is the coordinate of the interacting nucleon from T. Each of  $\mu$  and  $\nu$  denotes the  $z$ -component of isospin;  $1/2$  means neutron and  $-1/2$  does proton. The nonlocal  $U^{\text{EX}}$  has been localized in Eq. (2b) with the local semi-classical approximation [17], where  $\mathbf{K}(\mathbf{R})$  is the local momentum between P and T, and  $M = A/(1+A)$  for the target mass number  $A$ ; see Ref. [30] for the validity of the localization. The direct and exchange parts,  $g_{\mu\nu}^{\text{DR}}$  and  $g_{\mu\nu}^{\text{EX}}$ , of the  $g$ -matrix depend on the local density

$$\rho_{\mu\nu} = \rho_T^\nu(\mathbf{r}_T + \mathbf{s}/2) , \quad (3)$$

at the midpoint of the interacting nucleon pair; see Ref. [28] for the explicit forms of  $g_{\mu\nu}^{\text{DR}}$  and  $g_{\mu\nu}^{\text{EX}}$ .

The relative wave function  $\psi$  is decomposed into partial waves  $\chi_L$ , each with different orbital angular momentum  $L$ . The elastic  $S$ -matrix elements  $S_L$  are obtained from the asymptotic form of the  $\chi_L$ . The total reaction cross section  $\sigma_R$  is calculable from the  $S_L$  as

$$\sigma_R = \frac{\pi}{K^2} \sum_L (2L+1)(1 - |S_L|^2) . \quad (4)$$

The proton and neutron densities,  $\rho_p(r)$  and  $\rho_n(r)$ , are calculated with GHFB+AMP. As a way of taking the center-of-mass correction to the densities, we use the method of Ref. [28], since the procedure is quite simple.

## III. RESULTS

Figure 2 shows the proton  $\rho_p^{\text{GHFB}}$ , neutron  $\rho_n^{\text{GHFB}}$ , and matter  $\rho_m^{\text{GHFB}} \equiv \rho_p^{\text{GHFB}} + \rho_n^{\text{GHFB}}$  densities as a function of  $r$ . The experimental point-proton distribution extracted from the electron scattering data is also shown. The theoretical proton distribution  $\rho_p^{\text{GHFB}}$  reproduces the experimental  $\rho_p^{\text{exp}}$  reasonably well.

The Kyushu  $g$ -matrix folding model with the GHFB+AMP densities underestimates the  $\sigma_R$  data in  $30 \leq E_{\text{in}} \leq 100$  MeV only by a factor of 0.97, as shown in Fig. 3. The proton radius  $R_p^{\text{GHFB}} = 5.444$  fm calculated with GHFB+AMP agrees with the experimental value of  $R_p^{\text{exp}} = 5.444$  fm [42]. Because of  $\sigma_R \propto R_m^2$ , the observed discrepancy of  $\sigma_R$  is attributed to the underestimation of  $\rho_m^{\text{GHFB}}$  originating from the underestimation of  $\rho_n^{\text{GHFB}}$ . Small deviation makes it possible to scale the GHFB+AMP densities for the neutron density so as to reproduce  $\sigma_R^{\text{exp}}$  in  $E_{\text{in}} = 30\text{--}100$  MeV. The result of the scaling is  $R_n^{\text{exp}} = 5.722 \pm 0.035$  fm leading to

$$R_{\text{skin}}^{\text{exp}} = 0.278 \pm 0.035 \text{ fm.} \quad (5)$$

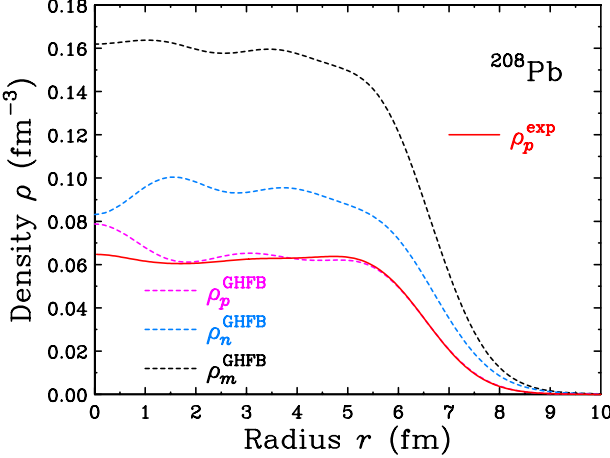


FIG. 2.  $r$  dependence of densities,  $\rho_p(r)$ ,  $\rho_n(r)$ ,  $\rho_m(r)$ , for  $^{208}\text{Pb}$  calculated with GHFB+AMP. Three dashed lines from the bottom to the top denote  $\rho_p(r)$ ,  $\rho_n(r)$ ,  $\rho_m(r)$ , respectively. The experimental point-proton (unfolded) density  $\rho_p$  is taken from Refs. [40, 41].

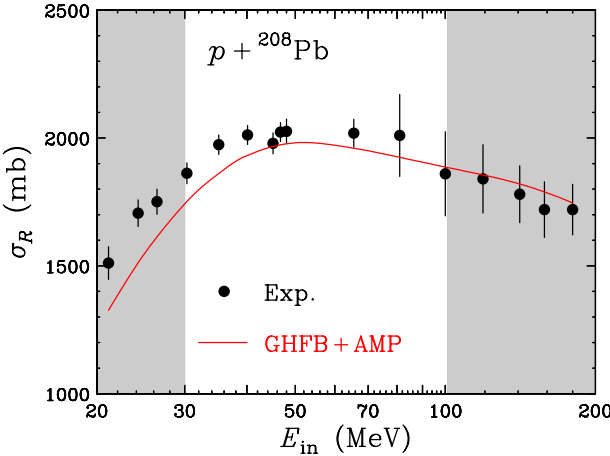


FIG. 3.  $E_{\text{in}}$  dependence of reaction cross sections  $\sigma_R$  for  $p + ^{208}\text{Pb}$  scattering. The solid line stands for the results of the Kyushu  $g$ -matrix folding model with GHFB+AMP densities. The data are taken from Refs. [37–39].

This result is consistent with  $R_{\text{skin}}^{PV} = 0.283 \pm 0.071$  fm.

Now we show a simple derivation of  $R_n^{\text{exp}}$  in the limit of  $K^{\text{exp}} = K^{\text{th}}$ . The experimental and theoretical (GHFB+AMP) reaction cross sections,  $\sigma_R^{\text{exp}}$  and  $\sigma_R^{\text{th}}$ , can be expressed as

$$\sigma_R^{\text{exp}} = K^{\text{exp}} \left[ (R_p^{\text{exp}})^2 \frac{Z}{A} + (R_n^{\text{exp}})^2 \frac{N}{A} \right], \quad (6a)$$

$$\sigma_R^{\text{th}} = K^{\text{th}} \left[ (R_p^{\text{th}})^2 \frac{Z}{A} + (R_n^{\text{th}})^2 \frac{N}{A} \right], \quad (6b)$$

where  $Z$ ,  $N$ , and  $A$  are proton, neutron, and atomic numbers of  $^{208}\text{Pb}$ , respectively, and  $K$  is a proportional coefficient between  $\sigma_R$  and  $R_m^2 = R_p^2(Z/A) + R_n^2(N/A)$ . By using  $K^{\text{exp}} = K^{\text{th}}$  and  $R_p^{\text{exp}} = R_p^{\text{th}}$ , the experimental neutron

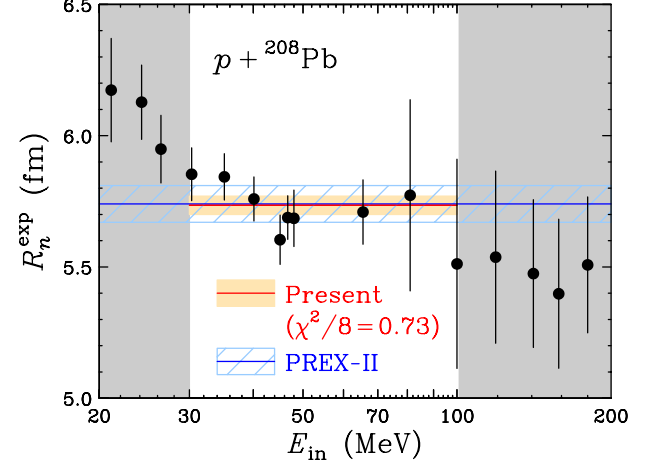


FIG. 4. Neutron radius  $R_n^{\text{exp}}$  of  $^{208}\text{Pb}$  deduced from the  $p + ^{208}\text{Pb}$  reaction cross section and the theoretical Kyushu  $g$ -matrix folding model calculations as a function of incident energy  $E_{\text{in}}$ .

radius  $R_n^{\text{exp}}$  can be deduced as

$$R_n^{\text{exp}} = \sqrt{\frac{Z(R_p^{\text{exp}})^2 + N(R_n^{\text{th}})^2}{N\sigma_R^{\text{th}}} \sigma_R^{\text{exp}} - (\sigma_p^{\text{exp}})^2 \frac{Z}{N}}, \quad (7)$$

from the experimental  $\sigma_R^{\text{exp}}$  and  $R_p^{\text{exp}}$  data and the theoretical  $R_n^{\text{th}}$  in GHFB+AMP.

Figure 4 shows the  $R_n^{\text{exp}}$  results as a function of incident energy  $E_{\text{in}}$ . The deduced  $R_n^{\text{exp}}$  values are almost independent of  $E_{\text{in}}$  in the region of  $E_{\text{in}} = 30$ –100 MeV where the present folding model is reliable [26]. By combining the eight data in this energy region, the neutron radius of  $^{208}\text{Pb}$  becomes  $R_n^{\text{exp}} = 5.735 \pm 0.035$  fm as shown by the filled band in Fig. 4. This result shows that the neutron skin thickness of  $^{208}\text{Pb}$  is  $R_{\text{skin}}^{\text{exp}} = 0.291 \pm 0.035$  fm with  $R_p^{\text{exp}} = 5.444$  fm [42]. The limit of  $K^{\text{exp}} = K^{\text{th}}$  is thus good, since  $R_{\text{skin}}^{\text{exp}} = 0.291 \pm 0.035$  fm is close to Eq.(5). Equation (7) is quite useful when  $\sigma_R^{\text{exp}} \approx \sigma_R^{\text{th}}$  and  $R_p^{\text{exp}} \approx R_p^{\text{th}}$ .

#### IV. SUMMARY

The proton radius  $R_p$  calculated with GHFB+AMP agrees with the precise experimental data of 5.444 fm. In  $30 \leq E_{\text{in}} \leq 100$  MeV, we can obtain  $r_n^{\text{exp}}$  from  $\sigma_R^{\text{exp}}$  by scaling the GHFB+AMP neutron density so as to reproduce  $\sigma_R^{\text{exp}}$  for each  $E_{\text{in}}$ , and take the weighted mean and its error for the resulting  $r_n^{\text{exp}}$ . From the resulting  $R_n^{\text{exp}} = 5.722 \pm 0.035$  fm and  $r_p^{\text{exp}} = 5.444$  fm, we can get  $R_{\text{skin}}^{\text{exp}} = 0.278 \pm 0.035$  fm.

In conclusion, our result  $R_{\text{skin}}^{\text{exp}} = 0.278 \pm 0.035$  fm is consistent with a new result  $r_{\text{skin}}^{208}(\text{PREX II}) = 0.283 \pm 0.071$  fm of PREX-II.

## ACKNOWLEDGMENTS

We would like to thank Dr. Toyokawa for providing his code.

- 
- [1] C. J. Horowitz, S. J. Pollock, P. A. Souder, and R. Michaels, Phys. Rev. C **63**, 025501 (2001).
- [2] S. Abrahamyan, Z. Ahmed, H. Albataineh, K. Aniol, D. S. Armstrong, W. Armstrong, T. Averett, B. Babineau, A. Barbieri, V. Bellini, *et al.* (PREX Collaboration), Phys. Rev. Lett. **108**, 112502 (2012).
- [3] C. J. Horowitz, Z. Ahmed, C.-M. Jen, A. Rakhman, P. A. Souder, M. M. Dalton, N. Liyanage, K. D. Paschke, K. Saenboonruang, R. Silwal, G. B. Franklin, M. Friend, B. Quinn, K. S. Kumar, D. McNulty, L. Mercado, S. Riordan, J. Wexler, R. W. Michaels, and G. M. Urciuoli, Phys. Rev. C **85**, 032501 (2012).
- [4] D. Adhikari, H. Albataineh, D. Androic, K. Aniol, D. S. Armstrong, T. Averett, S. Barcus, V. Bellini, R. S. Beminiwattha, J. F. Benesch, *et al.*, arXiv:2102.10767 [nucl-ex].
- [5] S. J. Novario, G. Hagen, G. R. Jansen, and T. Papenbrock, Phys. Rev. C **102**, 051303 (2020).
- [6] H. Shen, F. Ji, J. Hu, and K. Sumiyoshi, Astrophys. J. **891**, 148 (2020).
- [7] C. Horowitz, Ann. Phys. (Amsterdam) **411**, 167992 (2019).
- [8] Wei, Jin-Biao, Lu, Jia-Jing, Burgio, G. F., Li, Zeng-Hua, and Schulze, H.-J., Eur. Phys. J. A **56**, 63 (2020).
- [9] M. Thiel, C. Sfienti, J. Piekarewicz, C. J. Horowitz, and M. Vanderhaeghen, J. Phys. G: Nucl. Part. Phys. **46**, 093003 (2019).
- [10] B. T. Reed, F. J. Fattoyev, C. J. Horowitz, and J. Piekarewicz, arXiv:2101.03193 [nucl-th].
- [11] A. Trzcińska, J. Jastrzębski, P. Lubiński, F. J. Hartmann, R. Schmidt, T. von Egidy, and B. Kłos, Phys. Rev. Lett. **87**, 082501 (2001).
- [12] J. Zenihiro, H. Sakaguchi, T. Murakami, M. Yosoi, Y. Yasuda, S. Terashima, Y. Iwao, *et al.*, Phys. Rev. C **82**, 044611 (2010).
- [13] A. Tamii, I. Poltoratska, P. von Neumann-Cosel, Y. Fujita, T. Adachi, C. A. Bertulani, J. Carter, *et al.*, Phys. Rev. Lett. **107**, 062502 (2011).
- [14] C. M. Tarbert, D. P. Watts, D. I. Glazier, P. Aguar, J. Ahrens, J. R. M. Annand, H. J. Arends, R. Beck, V. Bekrenev, B. Boillat, *et al.* (Crystal Ball at MAMI and A2 Collaboration), Phys. Rev. Lett. **112**, 242502 (2014).
- [15] M. C. Atkinson, M. H. Mahzoon, M. A. Keim, B. A. Bordelon, C. D. Pruitt, R. J. Charity, and W. H. Dickhoff, Phys. Rev. C **101**, 044303 (2020).
- [16] I. Angelis and K. Marinova, At. Data Nucl. Data Tables **99**, 69 (2013).
- [17] F. Brieva and J. Rook, Nucl. Phys. A **291**, 299 (1977); Nucl. Phys. A **291**, 317 (1977); Nucl. Phys. A **297**, 206 (1978).
- [18] G. Satchler and W. Love, Physics Reports **55**, 183 (1979); G. R. Satchler, Direct Nuclear Reactions (Oxford University Press, 1983).
- [19] N. Yamaguchi, S. Nagata, and T. Matsuda, Prog. Theor. Phys. **70**, 459 (1983); S. Nagata, M. Kamimura, and N. Yamaguchi, Prog. Theor. Phys. **73**, 512 (1985); N. Yamaguchi, S. Nagata, and J. Michiyama, Prog. Theor. Phys. **76**, 1289 (1986).
- [20] K. Amos, P. J. Dortmans, H. V. von Geramb, S. Karatagliidis, and J. Raynal, “Nucleon-nucleus scattering: A microscopic nonrelativistic approach,” in Advances in Nuclear Physics, edited by J. W. Negele and E. Vogt (Springer US, Boston, MA, 2000) pp. 276–536.
- [21] T. Furumoto, Y. Sakuragi, and Y. Yamamoto, Phys. Rev. C **78**, 044610 (2008); Phys. Rev. C **79**, 011601 (2009); Phys. Rev. C **80**, 044614 (2009).
- [22] K. Egashira, K. Minomo, M. Toyokawa, T. Matsumoto, and M. Yahiro, Phys. Rev. C **89**, 064611 (2014).
- [23] M. Toyokawa, K. Minomo, M. Kohno, and M. Yahiro, J. Phys. G: Nucl. Part. Phys. **42**, 025104 (2014); J. Phys. G: Nucl. Part. Phys. **44**, 079502 (2017).
- [24] M. Toyokawa, M. Yahiro, T. Matsumoto, K. Minomo, K. Ogata, and M. Kohno, Phys. Rev. C **92**, 024618 (2015); Phys. Rev. C **96**, 059905(E) (2017).
- [25] M. Toyokawa, M. Yahiro, T. Matsumoto, and M. Kohno, Prog. Theor. Exp. Phys. **2018**, 023D03 (2018).
- [26] S. Tagami, M. Tanaka, M. Takechi, M. Fukuda, and M. Yahiro, Phys. Rev. C **101**, 014620 (2020).
- [27] K. Minomo, T. Sumi, M. Kimura, K. Ogata, Y. R. Shimizu, and M. Yahiro, Phys. Rev. Lett. **108**, 052503 (2012).
- [28] T. Sumi, K. Minomo, S. Tagami, M. Kimura, T. Matsumoto, K. Ogata, Y. R. Shimizu, and M. Yahiro, Phys. Rev. C **85**, 064613 (2012).
- [29] S. Watanabe, K. Minomo, M. Shimada, S. Tagami, M. Kimura, M. Takechi, M. Fukuda, D. Nishimura, T. Suzuki, T. Matsumoto, *et al.*, Phys. Rev. C **89**, 044610 (2014).
- [30] K. Minomo, K. Ogata, M. Kohno, Y. R. Shimizu, and M. Yahiro, J. Phys. G: Nucl. Part. Phys. **37**, 085011 (2010).
- [31] M. Toyokawa, K. Minomo, and M. Yahiro, Phys. Rev. C **88**, 054602 (2013).
- [32] M. Kohno, Phys. Rev. C **88**, 064005 (2013); Phys. Rev. C **96**, 059903(E) (2017).
- [33] H. V. von Geramb, K. Amos, L. Berge, S. Bräutigam, H. Kohlhoff, and A. Ingemarsson, Phys. Rev. C **44**, 73 (1991).
- [34] P. J. Dortmans and K. Amos, Phys. Rev. C **49**, 1309 (1994).
- [35] J. Fujita and H. Miyazawa, Prog. Theor. Phys. **17**, 360 (1957); Prog. Theor. Phys. **17**, 366 (1957).
- [36] M. Takechi, M. Fukuda, M. Mihara, K. Tanaka, T. Chinda, T. Matsumasa, M. Nishimoto, R. Matsumiya, Y. Nakashima, H. Matsubara, *et al.*, Phys. Rev. C **79**, 061601 (2009).
- [37] R. F. Carlson, A. J. Cox, J. R. Nimmo, N. E. Davison, S. A. Elbakr, J. L. Horton, A. Houdayer, A. M. Sourkes, W. T. H. van Oers, and D. J. Margaziotis, Phys. Rev. C **12**, 1167 (1975).
- [38] A. Ingemarsson, J. Nyberg, P. Renberg, O. Sundberg, R. Carlson, A. Auce, R. Johansson, G. Tibell, B. Clark, L. Kurth Kerr, and S. Hama, Nucl. Phys. A **653**, 341 (1999).
- [39] A. Auce, A. Ingemarsson, R. Johansson, M. Lantz, G. Tibell, R. F. Carlson, M. J. Shachno, A. A. Cowley, G. C. Hillhouse, N. M. Jacobs, *et al.*, Phys. Rev. C **71**, 064606 (2005).
- [40] H. De Vries, C. De Jager, and C. De Vries, At. Data Nucl. Data Tables **36**, 495 (1987).
- [41] H. Euteneuer, J. Friedrich, and N. Voegler,

Nucl. Phys. A **298**, 452 (1978).

[42] A. B. Jones and B. A. Brown, Phys. Rev. C **90**, 067304 (2014).